

# Strongly coupled $\Upsilon(1S)$ suppression in $\sqrt{s}_{NN} = 2.76$ TeV Pb+Pb collisions

N N Barnard and W A Horowitz

Department of Physics, University of Cape Town, Private Bag X3, Rondebosch 7701, South Africa

E-mail: brnnad007@myuct.ac.za

**Abstract.** In a revolutionary paper, Matsui and Satz proposed using the suppression of quarkonia as a smoking gun signature of deconfinement in relativistic heavy ion collisions. The stunning success of using strong-coupling, AdS/CFT techniques to predict the viscosity to entropy density ratio extracted from RHIC and LHC heavy ion collision data using sophisticated 3+1D relativistic viscous hydrodynamics has prompted further investigation into the physics of a strongly-coupled plasma. We compute, for the first time, the suppression of bottomonia in a strongly coupled QGP, and compare the results to those from a weakly coupled QGP and to data. The complex binding energies which inform the thermal width and hence the  $R_{AA}$  of  $\Upsilon(1S)$  are determined using imaginary time techniques.

## 1. Introduction

The relativistic heavy-ion collisions at the Large Hadron Collider (LHC) and the Relativistic Heavy Ion Collider (RHIC) are sufficiently energetic for hadrons to transition into a new phase of colored matter, known as the quark-gluon plasma (QGP) [1]. Quarkonia may theoretically exist in conjunction with the QGP at  $T > T_c$ , where  $T_c$  is the critical temperature required for QGP formation, due to its small binding radii relative to the screening radius. At some  $T$ , the screening radius becomes smaller than the typical quarkonia radii, leading to their dissolution. In addition, excited states of quarkonia dissociate before the ground state [2]. The suppression of the bound states of quarkonia in heavy-ion collisions is hence considered a valuable indicator of the formation of QGP, and the comparison of this suppression to that in minimum bias  $p + p$  collisions where no QGP is formed, is a useful probe of the QGP's properties.

Potential models can be used to describe the interaction of the quark and antiquark in the  $q\bar{q}$  pair to calculate the suppression of quarkonia production in heavy-ion collisions [3]. This potential at finite temperature contains not only a standard real Debye-screened term, but also an imaginary part which gives the thermal width of the state, and hence its suppression [4]. One of the first to show this was [5], which made use of perturbative methods to find the static potential of quarkonia at finite temperature. They concluded that the thermal width of the state increases with  $T$ , suggesting that at high  $T$  the dissociation due to the effect described by the imaginary part of the potential occurs before color screening can even come into effect.

The complex-valued potential was explored further using non-perturbative lattice QCD by [4], among others, allowing for the study of strongly-coupled quarkonia as well. An important consideration in finding heavy quarkonium suppression is the velocity of the  $q\bar{q}$  in relation to the

surrounding QGP, however, while perturbative and lattice QCD calculations generally consider the  $q\bar{q}$  meson to be at rest in the medium.

The suppression of quarkonia moving at velocity in a QGP hence requires holographic techniques such as the Anti-de Sitter/Conformal Field Theory (AdS/CFT) correspondence. The potential for static quarkonia at finite temperature in  $\mathcal{N} = 4$  super Yang-Mills theory was calculated by [6, 7, 8], among others. Liu, Rajagopal and Wiedemann (LRW) [9] were the first to present a quantitative description from AdS/CFT of the consequences of velocity on the screening length of charmonium, suggesting that for strongly coupled  $J/\psi$ , velocity could result in a significant additional source of suppression at high transverse momentum  $p_T$  in the form of a decrease in dissociation energy with increased velocity. Since then, many have performed similar investigations, and while the aforementioned are limited in their scope of application, it is interesting to note that [10] in particular concludes that the effect of velocity may not be as consequential as postulated in LRW.

On the other hand, from pQCD, [11] found a potential for weakly coupled  $q\bar{q}$  states which is dependent on velocity and shows that the dissociation energy increases with quarkonia velocity.

We would ultimately like to investigate the consequences of these different velocity dependence pictures from AdS/CFT compared to pQCD. Here we have a more modest goal: to compare the suppression of quarkonia at rest with respect to the QGP for pQCD vs. AdS/CFT potentials.

We consider the case of ground state bottomonia at rest with respect to an isotropic quark-gluon plasma. We follow the methodology outlined in Krouppa et al. [12], with a number of improvements. Given a potential, we evolve a random wave function through imaginary time; after a sufficiently long evolution, only the ground state wave function remains. This ground state wave function then determines the ground state binding energy. We independently confirmed these binding energies by an application of the complex Ritz variational method [13]. Finally, following Krouppa, we used the complex binding energies in a quarkonia suppression model to compute  $R_{AA}$ .

## 2. Methodology

### 2.1. Potential Models

The potential model presented here for weakly coupled quarkonia is taken from [12] and is complex-valued. Both the real and the imaginary parts of the potential were found using leading-order perturbative calculations. We show the real part and imaginary part of the potential  $V(r)$  as a function of quark separation  $r$  in figure 1a and figure 1b, respectively.

We modeled the strongly coupled quarkonia at rest in a QGP with the potential given in Albacete et al. [6]. In that work, the authors derive the potential in  $\mathcal{N} = 4$  super Yang-Mills at finite temperature using AdS/CFT. Figures 2a and 2b show the real and imaginary parts of  $V_s(r)$  as a function of quark separation  $r$ , taking the 't Hooft coupling  $\lambda = 10$ . See [14] for full functional forms of the potential models.

Note that the real parts of the pQCD and AdS/CFT potentials, shown in figures 1a and 2a, respectively, are similar in form, but the imaginary parts from pQCD and AdS/CFT, shown in figures 1b and 2b, respectively, differ greatly: the imaginary part of the pQCD potential saturates as a function of  $r$  whereas that of the AdS/CFT potential diverges.

### 2.2. Numerical Integration of TDSE

The methodology used here follows that of [12, 15], adapted to the special case of an isotropic plasma, with various modifications of the discretization (see [14] for details). In order to compute the ground state wave function, and hence the binding energy, we need to solve the non-relativistic, time dependent Schrödinger Equation (nRTDSE):

$$i\partial_t\Psi(r, t) = H\Psi(r, t). \tag{1}$$

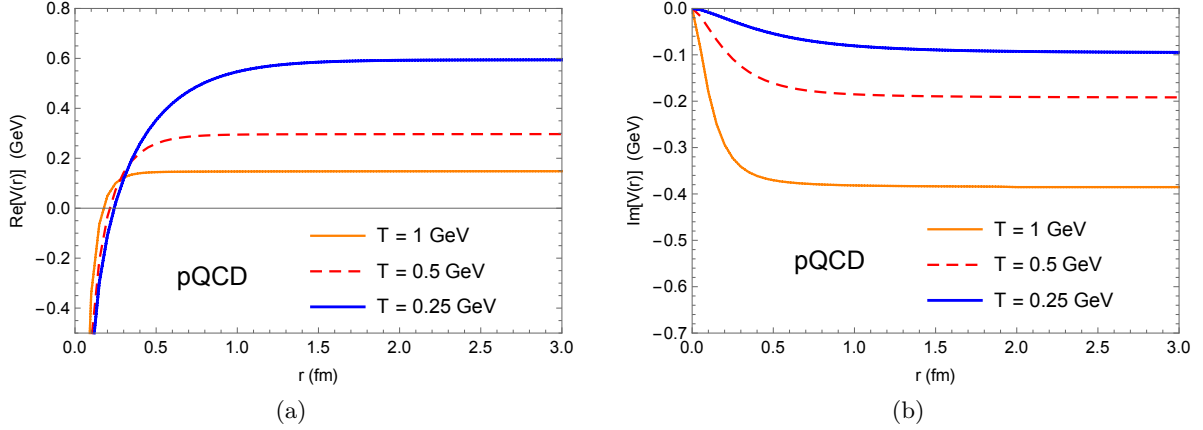


**Figure 1.** The (a) real part of the weakly coupled potential  $\Re[V(r)]$ , and the (b) imaginary part of the potential  $\Im[V(r)]$ , as a function of the distance  $r$  between the quark and anti-quark in the  $b\bar{b}$ , for various  $T$  in an isotropic plasma.

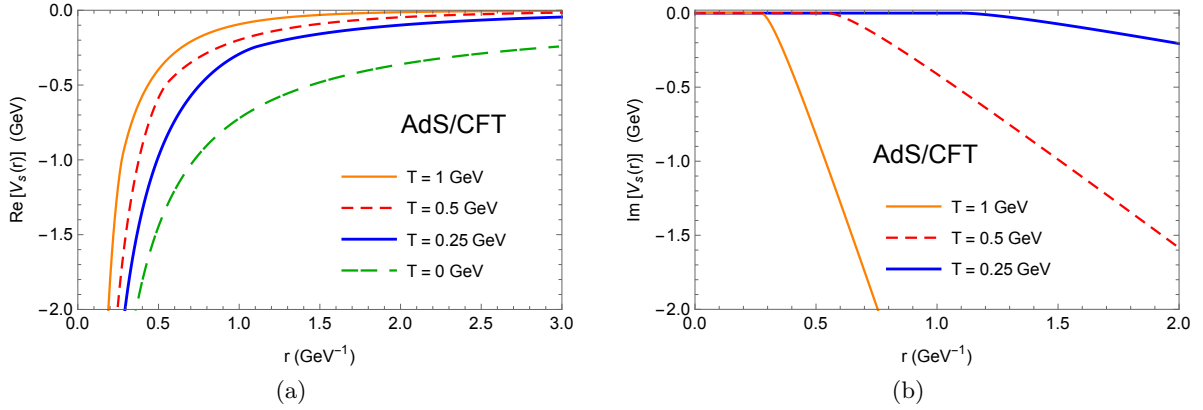


**Figure 2.** The (a) real part of the strongly coupled potential  $\Re[V_s(r)]$  and the (b) imaginary part of the potential  $\Im[V_s(r)]$  as a function of the distance  $r$  between the quark and anti-quark in the  $b\bar{b}$ , for various temperatures  $T$  in an isotropic plasma.

Performing a Wick rotation to an imaginary time  $\tau \equiv it$ , Eq. (1) has the general solution

$$\Psi(r, \tau) = \sum_{n=0}^{\infty} c_n \psi_n(r) e^{-E_n \tau}. \quad (2)$$

Since  $E_n > E_0$  for all  $n > 0$ , one can evolve forward in imaginary time such that all the higher order wave functions are suppressed and only the ground state wave function remains:

$$\lim_{\tau \rightarrow \infty} \Psi(r, t) \rightarrow c_0 \psi_0(r) e^{-E_0 \tau}, \quad (3)$$

where  $\psi_0(r)$  is the ground state wave function and  $E_0$  the ground state energy. The binding energy of the state can then be found from

$$E_{\text{bind}} \equiv E_0 - \Re[V(|r| \rightarrow \infty)], \quad (4)$$

where the ground state energy  $E_0$  can be found from the ground state wave function,

$$E_0 = \frac{\int r^2 dr \psi_0(r)^* H \psi_0(r)}{\int r^2 dr |\psi_0|^2}. \quad (5)$$

### 2.3. Suppression

We would like to make quantitative predictions for the suppression of bottomonia in heavy ion collisions and compare to measured data. The nuclear modification factor  $R_{AA}$  is calculated following [12]:

$$R_{AA}(p_T, y, \mathbf{x}_\perp, b) = e^{-\zeta(p_T, y, \mathbf{x}_\perp, b)}, \quad (6)$$

$$\zeta \equiv \Theta(\tau_f - \tau_{\text{form}}) \int_{\max(\tau_{\text{form}}, \tau_0)}^{\tau_f} d\tau \Gamma(\tau, \mathbf{x}_\perp, \varsigma = y),$$

where the thermal width  $\Gamma(\tau, \mathbf{x}_\perp, \varsigma)$  is given as

$$\Gamma(\tau, \mathbf{x}_\perp, \varsigma) = \begin{cases} -2\Im[E_{\text{bind}}] & \Re[E_{\text{bind}}] < 0 \\ \gamma_{\text{dis}} & \Re[E_{\text{bind}}] \geq 0. \end{cases} \quad (7)$$

We take  $\gamma_{\text{dis}} = 10$  GeV, as was done in [12]. Furthermore,  $b$  is the impact parameter, and  $y$  the rapidity, taken to be zero. The formation time  $\tau_{\text{form}}$  is calculated using

$$\tau_{\text{form}} = E_T \tau_{\text{form}}^0 / m_Q \quad (8)$$

where  $\tau_{\text{form}}^0 = 0.2$  fm is taken for the initial formation time of the state [12]. Lastly, the final time  $\tau_f$  is taken as the time at which the temperature  $T$  of the QGP drops below the critical temperature  $T_c$ .

We use the optical limit of the Glauber model [16] to describe the background in the case of  $\sqrt{s_{\text{NN}}} = 2.76$  TeV Pb+Pb collisions. Taking a weighted average over the region with limits  $\mathbf{x}_\perp = [-10, 10]$  fm, we have

$$R_{AA}(p_T, b) = \frac{\int d^2\mathbf{x}_\perp d\phi T_{AA}(\mathbf{x}_\perp, b) R_{AA}(p_T, y, \mathbf{x}_\perp, b)}{2\pi N_{\text{coll}}}, \quad (9)$$

where  $T_{AA}(\mathbf{x}_\perp, b)$  is the nuclear overlap function and  $N_{\text{coll}} \equiv \int d^2\mathbf{x}_\perp T_{AA}(\mathbf{x}_\perp, b)$  is the number of binary nucleon-nucleon collisions in the region. We set a central temperature  $T_0 = 522$  MeV and initial formation time  $\tau_0 = 0.3$  fm, as is done in [12].

## 3. Results

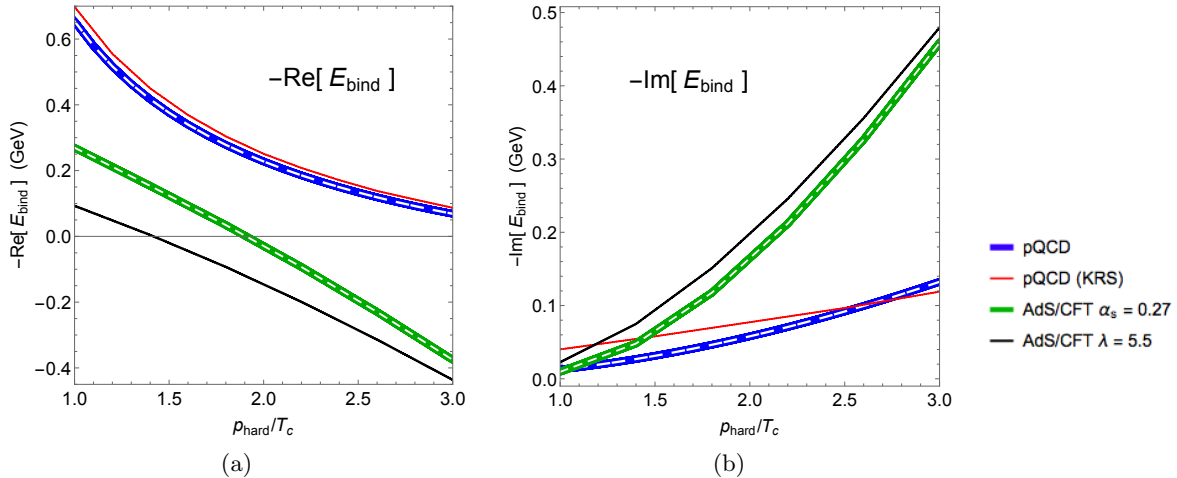
### 3.1. Binding Energies

Figure 3a gives the real part of the binding energy of  $\Upsilon(1S)$  from the pQCD potential, and strongly coupled potential, as a function of temperature. Similarly, figure 3b gives the imaginary part of the binding energies for all cases mentioned above. The binding energy results for weakly coupled bottomonium from [15] are labeled ‘‘pQCD (KRS)’’ and are included for comparison.

For the AdS/CFT results, we show the binding energy, both for the case where the coupling constant is  $\lambda = 10$  (labeled as  $\alpha_s = 0.27$ ) and where  $\lambda = 5.5$ , in an attempt to at least partially map out some of the systematic theoretical uncertainties associated with the use of the AdS/CFT correspondence – this is discussed in section 3.2.

Both the binding energy results presented for the pQCD potential and the AdS/CFT potential taking  $\lambda = 10$  were independently confirmed using a complex variational method, further explained in [14].

The binding energy found from our adapted methodology for the pQCD potential differs quantitatively from that presented in [15], which was used in Krouppa et al. [12] to calculate suppression. In the case of  $\Upsilon(1S)$ , this difference does not change the qualitative behavior of the quarkonia, since both results suggest that the quarkonia remain bound up to at least  $T = 3T_c$ .



**Figure 3.** The (a) negative real part of  $E_{\text{bind}}$  and (b) negative imaginary part of  $E_{\text{bind}}$  for  $\Upsilon(1S)$ . The blue, green, and black curves give the results for weakly coupled and strongly coupled ( $\lambda = 10$  and  $\lambda = 5.5$ )  $\Upsilon(1S)$ , respectively. The dashed white curves are from the independent evaluation using a complex variational method. The results from KRS [15], which should be identical to the blue curves, are given as solid red for comparison.

However, we see in the results that follow that the small quantitative differences in the derived binding energies lead to a significant quantitative difference in the predicted suppression.

The imaginary part of the binding energies from AdS/CFT are notably larger than those of weakly coupled quarkonia, and rise more steeply. This result is not surprising as the AdS/CFT potential has a divergent imaginary part, compared to the saturation of the imaginary part of the pQCD potential.

Unlike in the case of the weakly coupled quarkonia where the  $\Upsilon(1S)$  remains bound for the temperature range considered, the strongly coupled  $\Upsilon(1S)$  dissociates at  $\sim 1.9T_c$ . The comparatively larger imaginary part of the binding energy up to the temperature at which the bottomonium dissociates implies a much larger thermal width at higher  $T$ , and hence a larger suppression.

### 3.2. Suppression

Figure 4a gives the nuclear modification factor  $R_{AA}$  for each of the sets of binding energies shown in figure 3a and 3b as a function of the number of participating nucleons  $N_{\text{part}}$ . To this end, the  $R_{AA}(p_T, b)$  from Eq. (9) is averaged over the transverse momentum range  $0 \leq p_T \leq 40$  with a weighting of  $E^{-4}$  [12].

Figure 4b shows  $R_{AA}(p_T)$ , where all centrality classes are included, weighed by the number of binary nucleon-nucleon collisions  $N_{\text{coll}}$ . Suppression results for mid-rapidity ( $|y| < 2.4$ ) Pb+Pb collisions at  $\sqrt{s_{NN}} = 2.76$  TeV from the CMS Collaboration [17] are included in figure 4a and 4b for comparison.

We show in figures 4a and 4b two predictions for the suppression of strongly coupled bottomonia. Since we used a potential derived in AdS-space dual to maximally supersymmetric Yang-Mills theory, there is no single obvious map between the parameters of QCD and of  $\mathcal{N} = 4$  SYM. For the  $\alpha_s = 0.27$  curve, we took  $\lambda_{SYM} = 10$  and  $T_{SYM} = T_{QCD}$ , where  $\lambda_{SYM} = 10 = \sqrt{4\pi\alpha_s N_c}$  (and thus  $\alpha_s = 0.27$  for  $N_c = 3$ ) is approximately the value of the QCD running coupling constant evaluated at the first Matsubara frequency of the plasma. For the  $\lambda = 5.5$  curve, the coupling constant was set by a comparison to the  $q\bar{q}$  potential from lattice and  $T_{SYM} = T_{QCD}/3^{-1/4}$  is a result of assuming the entropies of the QCD and SYM plasmas are the same [18].

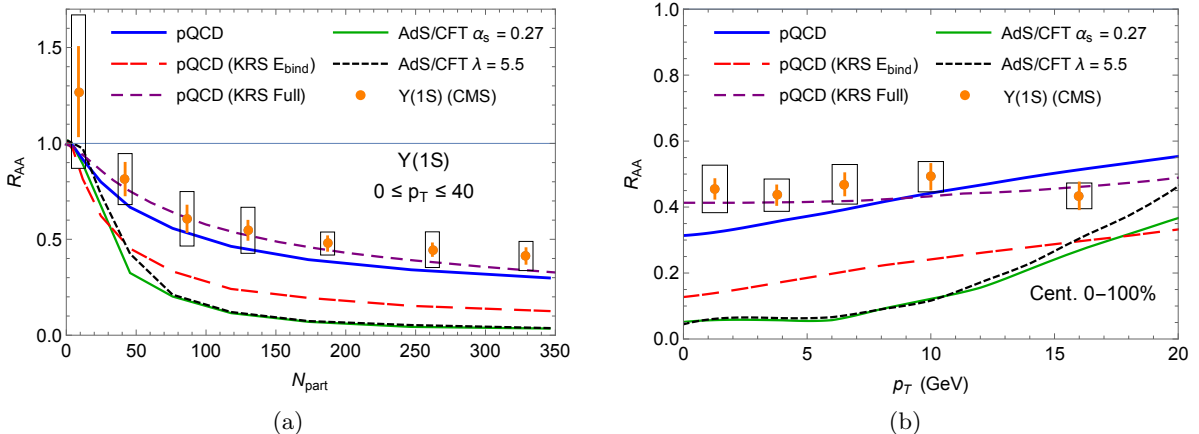


**Figure 4.** (a) Nuclear modification factor  $R_{AA}$  as a function of the number of participating nucleons  $N_{part}$  for  $0 \leq p_T \leq 40$ . (b) Nuclear modification factor  $R_{AA}$  as a function of transverse momentum  $p_T$  for combined centrality classes. In both subfigures, the thick solid blue line gives our results for weakly coupled  $\Upsilon(1S)$ , and the dashed-dotted red line that calculated for the binding energy from KRS [15] using our suppression model. The  $R_{AA}$  presented in KRS [12] as calculated using their suppression model is given in dashed purple. The solid green and dotted black lines give the results for strongly coupled  $\Upsilon(1S)$  with coupling constants  $\alpha_s = 0.27$  (and  $T_{SYM} = T_{QCD}$ ) and  $\lambda = 5.5$  (and  $T_{SYM} = T_{QCD}/3^{1/4}$ ), respectively. Data from CMS [17] is included in orange.

We show in figures 4a and 4b three predictions for weakly coupled bottomonia: 1) the suppression using the binding energies we compute from the potential in [15] run through our medium background, 2) the suppression using the binding energies computed in [15] run through our medium background, and 3) the suppression quoted in [12] in which they run the binding energies computed in [15] through their background.

#### 4. Discussion and Outlook

We computed for the first time the suppression of bottomonia in an isotropic strongly coupled QGP and compared the results to those from a weakly coupled QGP and to data from the CMS Collaboration [17].

The non-relativistic, time dependent, radially symmetric Schrödinger Equation was solved numerically in order to find the ground state wave functions for two potential models: one from pQCD and one from AdS/CFT. The numerical evaluation of the imaginary time Schrödinger Equation was performed by evolving forward in imaginary time until all higher order wave functions were sufficiently suppressed. The potential used for weakly coupled quarkonia was taken from [15], in which the potential came from leading-order pQCD with various corrections. The strongly coupled quarkonia potential was taken from [6], who obtained their potential from AdS/CFT.

The ground state wave functions obtained were then used to find the (complex) ground state energies for  $\Upsilon(1S)$ . These ground state energies were then independently confirmed using a complex variational technique [13]. Our binding energies for the weakly coupled potential in [15] differed somewhat from those found in [15], likely due to extending the physical region under consideration and from a possibly more careful treatment of the potential.

Our first results for  $\Upsilon(1S)$  strongly coupled to a strongly coupled plasma show binding energies with much larger imaginary parts than those found from the pQCD potential, as well as real parts that become positive within the  $T_c$  to  $3T_c$  range considered. Thus, for the potential

models considered here, a strongly coupled  $\Upsilon(1S)$  interacting with a strongly coupled plasma melts at a *lower temperature* than a weakly coupled  $\Upsilon(1S)$  interacting with a weakly coupled plasma. The  $\Upsilon(1S)$  hence appears more strongly bound at weak coupling than at strong coupling, which is surprising.

Since the weak coupling bottomonia become more strongly bound as the coupling is increased and the strong coupling bottomonia become less strongly bound as the coupling decreases, that the weak coupling bottomonia is more strongly bound at weak coupling than at strong coupling suggests some non-monotonic behavior of the binding energies at the threshold between the weak and strong coupling regimes. This non-monotonic behavior possibly stems from deriving the potential at weak coupling in QCD whereas the strong coupling potential was derived in the slightly different theory,  $\mathcal{N} = 4$  SYM; it would be interesting to compare binding energies from the quarkonium potential at weak and strong coupling consistently within  $\mathcal{N} = 4$  SYM.

We then input the complex ground state binding energies we found using the imaginary time techniques into an implementation of the suppression model described in [12] to determine the  $\Upsilon(1S)$  nuclear modification factor  $R_{AA}$  as a function of the number of participating nucleons,  $N_{\text{part}}$ , and of transverse momentum,  $p_T$ , respectively. The difference in binding energies for the two coupling scenarios is echoed in the  $R_{AA}$  results: from the larger imaginary parts of the strongly coupled binding energies, we see a significantly larger suppression for strongly coupled  $\Upsilon(1S)$  than for weakly coupled  $\Upsilon(1S)$ . Quantitatively, our full model—comprised of the potential, the resulting quarkonia binding energies, and the translation to  $R_{AA}$ —significantly overpredicts the suppression of strongly coupled bottomonia compared to data. At the same time, our predictions for weakly coupled bottomonia are consistent with data.

We note that our model for the medium is significantly less sophisticated compared to that used in [12]: our background is an optical Glauber model as opposed to the 3+1D viscous anisotropic hydrodynamics in that work. Our medium incorporates only Bjorken expansion, whereas the background in [12] includes transverse expansion and entropy production. Therefore the plasma in [12] cools faster than ours, leading to our model showing more dissociation for the same binding energies. The extent of the sensitivity of  $R_{AA}$  to the background used is surprisingly large. With the only difference being the background geometry used, we ran the binding energies from [15] through our suppression model and found an  $R_{AA}$  a factor of two smaller than that shown in [12].

In contrast to the favorable comparison between the pQCD-based results of [12] and the CMS data [17], if we assume our weak coupling binding energies are more accurate than those of [15], then computing  $R_{AA}$  with the more sophisticated background from [12] would likely yield a significant underprediction of the suppression of bottomonia.

At strong coupling, with a potential derived from AdS/CFT as described in [6], it seems unlikely that the use of a more sophisticated background would reduce the suppression of bottomonia enough that the predicted  $R_{AA}$  would be consistent with data; however, the differences from using a more sophisticated background, suppression model, and velocity dependent potential may ultimately be sufficient for future strongly coupled quarkonia predictions to be consistent with current data.

We note that our suppression calculations do not consider feed-down from higher excited states  $\Upsilon(nS)$ ,  $n > 1$  for either the pQCD or AdS/CFT potentials. Considering feed-down, however, would only serve to suppress the  $R_{AA}$  further. Hence, our qualitative conclusions about strongly-coupled quarkonia would remain unchanged should higher excited states be included.

We leave the implementation of more advanced calculations of quarkonia suppression—including better modeling of the medium background, more accurate initial quarkonia production, a more realistic dissociation model, and the use of velocity dependent potentials—and a more thorough investigation of systematic theoretical uncertainties in quarkonia  $R_{AA}$  for future work.

## Acknowledgments

The authors wish to thank the South African National Research Foundation and the SA-CERN Consortium for their financial support.

## References

- [1] Gyulassy M and McLerran L 2005 *Nucl. Phys. A* **750** 30–63
- [2] Karsch F, Kharzeev D and Satz H 2006 *Phys. Lett. B* **637** 75–80
- [3] Matsui T and Satz H 1986 *Phys. Lett. B* **178** 416–22
- [4] Rothkopf A, Hatsuda T and Sasaki S 2012 *Phys. Rev. Lett.* **108** 162001
- [5] Laine M, Philipsen O, Romatschke P and Tassler M 2007 *J. High Energy Phys.* JHEP03(2007)054
- [6] Albacete J L, Kovchegov Y V and Taliotis A 2008 *Phys. Rev. D* **78** 115007
- [7] Noronha J and Dumitru A 2009 *Phys. Rev. Lett.* **103** 152304
- [8] Ewers C, Kaczmarek O and Samberg A 2016 arXiv:1605.07181
- [9] Liu H, Rajagopal K and Weidemann U A 2007 *Phys. Rev. Lett.* **98** 182301
- [10] Finazzo S I and Noronha J 2015 *J. High Energy Phys.* JHEP01(2015)051
- [11] Escobedo M A, Giannuzzi F, Mannarelli M and Soto J 2013 *Phys. Rev. D* **87** 114005
- [12] Krouppa B, Ryblewski R and Strickland M 2015 *Phys. Rev. C* **92** 061901
- [13] Kraft D and Plessas W 2016 *J. Phys.: Conf. Ser.* **738** 012029
- [14] Barnard N N and Horowitz W A 2017 arXiv:1706.09217
- [15] Margotta M, McCarty K, McGahan C, Strickland M and Yager-Elorriaga D 2011 *Phys. Rev. D* **83** 105019
- [16] Miller M L, Reygers K, Sanders S J and Steinberg P 2007 *Ann. Rev. Nucl. Part. Sci.* **57** 205–43
- [17] Khachatryan V *et al* (CMS) 2017 *Phys. Lett. B* **770** 357–9
- [18] Gubser S S 2008 *Nucl. Phys.* **B790** 175–199